

Electronic structure of a Ti(0001) film

Peter J. Feibelman

Sandia Laboratories, Albuquerque, New Mexico 87185*

J. A. Appelbaum and D. R. Hamann

Bell Laboratories, Murray Hill, New Jersey 07974

(Received 1 March 1979)

A self-consistent calculation of the electronic structure of a thin Ti(0001) film leads to the prediction of a band of surface states coincident with the Fermi level and extending a few tenths of an eV on either side of it. The calculation is performed in a linear combination of Gaussian orbitals basis. The procedure by which the evaluation of the Hamiltonian matrix is reduced to summing over three-center integrals as well as the method by which Gaussian bases are selected are thoroughly described. Observation of the predicted surface band by angle-resolved photoemission is discussed, as well as the question of how general a surface band near the Fermi energy should be among the hcp d -band metals. A shift of surface atom core levels to 0.25 eV greater binding energy is predicted, and the origin of this shift is discussed.

I. INTRODUCTION

Recent work has shown that calculation of the surface electronic structure of d -band materials is within the power of present day computational techniques.¹⁻⁶ It is therefore timely to begin a study of the systematics of surface electronic properties across the Periodic Table. Among the $3d$ metals self-consistent surface-electronic-structure calculations have been performed only for Cu,¹ and Ni.² (For the $4d$'s the list includes Nb,³ Mo,⁴ Pd,⁵ and Ag.⁶) Accordingly we present here the results of a self-consistent calculation of the electronic properties of a thin (11-layer) Ti(0001) film.

Our numerical method is based on a linear combination of Gaussian orbitals approach, which permits the analytic evaluation of the many integrals that enter the Hamiltonian matrix. The only physical (as opposed to numerical) approximation we make is the assumption of a local exchange-correlation potential. The data required for the calculation comprise the locations of the Ti atoms and the assumed (Wigner interpolation) form of the local exchange-correlation potential. Thus our results are parameter free.

The most striking result of our calculation is shown in Fig. 1. The density of states in the lower d -band region narrows dramatically at the surface. This is due primarily to a quite narrow band of surface states found to coincide with the Ti Fermi energy, extending no more than a few tenths of an eV on either side of it. This result suggests that occupation of the surface band plays a large role in determining the strength of the dipole layer at the Ti surface, and hence the Ti(0001) work function (which we find to

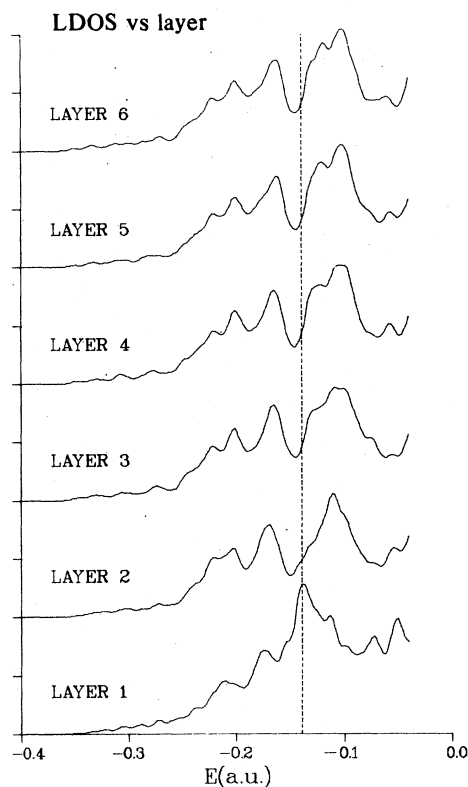


FIG. 1. Layerwise local density of states (LDOS) for an 11-layer Ti(0001) film. The vacuum level is at energy 0.0. The dotted line indicates the Fermi level at $E = -0.139$ a.u. ($= -3.8$ eV). Note the strong surface resonance in the outermost ("1st") layer.

be 3.8 eV, in good agreement with experiment⁷). However further calculations are required to see whether the coincidence of the Fermi energy with a surface band is a general feature of the surfaces of hcp *d*-band metals, or is simply an accident in the case of Ti(0001). We also find a core-level shift of 0.25 eV greater binding energy for surface atom core states than for bulk core states. This is a shift in the opposite direction to that previously found for Cu(111) in similar calculations.⁶

The remainder of this article is divided into two main parts. First we review⁸ the scheme by which the Schrödinger equation for the film is reduced to a form suitable for numerical computation. Then we present our results for Ti in detail, focusing on the possibility of observing the predicted surface states in angle-resolved photoemission.

II. NUMERICAL APPROXIMATION METHOD

In this section we discuss the calculation of electronic structure by means of a linear combination of localized orbitals approach.

Once one decides to represent one's wave function as a linear combination of localized orbitals it becomes plain that a major task involved in numerical computation is in evaluating the integrals that enter the Hamiltonian (and, if the orbitals are not orthogonalized, the overlap) matrix. In order to reduce this expense, the obvious procedure is to choose Gaussians (or "contracted" Gaussians⁹) as the localized orbitals, since multicenter integrals over Gaussians can be performed analytically.

However if one is attempting a self-consistent calculation, the choice of a Gaussian basis for the wave functions is not sufficient to reduce the Schrödinger equation to a manageable form. Consider for example the evaluation of the matrix elements of the electrostatic potential. Such matrix elements are in general *four*-center integrals, since they contain initial and a final wave functions as well as the charge density, which, in a self-consistent calculation, is a sum of squares of linear combinations of Gaussian orbitals. Although the evaluation of four-center integrals can be carried out analytically for Gaussian orbitals, the number of such integrals that must be stored and summed would be prohibitively large. The convergence of direct lattice sums for multipole potentials is also unacceptably slow.

Problems also exist in evaluating the matrix elements of the exchange-correlation potential. This potential is generally taken, in the local approximation, to be a nonlinear function of the charge density $n(\vec{r})$, e.g., $\text{const.} \times n^{1/3}(\vec{r})$. Thus the matrix elements of the exchange-correlation potential cannot be evaluated analytically even if a Gaussian wave-function basis is used.

The method that we have adopted to avoid these difficulties was first discussed by Sambe and Felton¹⁰ in the context of molecular calculations. We choose, in addition to the Gaussian wave-function basis, a separate Gaussian basis to represent the spatial variation of the charge density and self-consistent potential. Given a charge density expressed in this form, the least-squares fit to the corresponding electrostatic potential can be carried out after a manageable number of analytic integrals are computed. A modified Ewald technique enables the long-range potential to be handled analytically in Fourier space. Evaluating and fitting the exchange-correlation potential on a real-space mesh is also tractable. Once the self-consistent potential is represented as a linear combination of Gaussians, the evaluation of the Hamiltonian matrix requires no worse than three-center analytic integrals, and therefore becomes a manageable problem. Least-square fitting this basis to the exact charge, which is the Brillouin-zone sum of the squares of the occupied wave functions, requires precisely the same integrals. On the other hand we are now faced with a new issue, namely, deciding what constitutes an *adequate* basis for the charge density and the potential.

Ideally, the integrated square error of the large fit should be evaluated and used as a figure of merit. This procedure involves sums of four-center integrals, however, and has not been practical to carry out. Therefore we have made use of two somewhat less stringent criteria to establish the adequacy of a given charge and potential basis. The first is the global requirement of charge conservation. That is we require that the unconstrained least-squares fit to the exact charge-density result in a fitted charge density which has very close to the correct number of electrons per unit cell. Typically in our Ti calculations the quality of the charge-density fit did not vary appreciably from iteration to iteration as self-consistency was approached. The basis used in obtaining the results presented below permitted a charge fit that was accurate to 1×10^{-4} in the total charge per cell. It should be noted that although an *unconstrained* fit of the exact charge to the charge basis was performed after each iteration, a fit that was *constrained to give exact charge conservation* was used in order to evaluate the potential. In this way divergences associated with nonsatisfaction of overall charge neutrality are avoided. The second criterion is the requirement that the fitted charge be sensibly behaved in real space.

When it comes to choosing an adequate charge and potential basis for a film, the most difficult additional problem is representing the charge as it drops to zero in the vacuum region. If the basis is chosen poorly, the fitted electron number density will show unphysical oscillations¹¹ and even become negative at a distance from the surface atomic layer where the planar

average number density is not yet particularly small. In order to ensure that basis-dependent, unphysical charge-density oscillations are adequately suppressed in the vacuum region we evaluate the fitted spatial charge distribution explicitly. The charge basis we finally used for Ti was deemed satisfactory in that the contours of constant charge became fairly flat as one left the surface and remained flat out to a distance of about 4 a.u. beyond the surface atomic layer (see Fig. 2). At this distance the charge density was ~ 0.002 electrons/a.u.³ compared to an average bulk Ti valence charge density of 0.034 electrons/a.u.³. The work function associated with the self-consistent fitted charge density turned out to equal 3.8 eV. The agreement of this value with experimental values, ~ 4 eV,⁷ is at least partial confirmation that our basis, which accurately represents the falloff of the valence charge density down to $\sim \frac{1}{20}$ its bulk average value, is an adequate one.

To complete the description of our calculation we turn now to the specifics of our wave-function and charge-potential Gaussian bases. By assumption the valence wave functions for a Ti film are written in

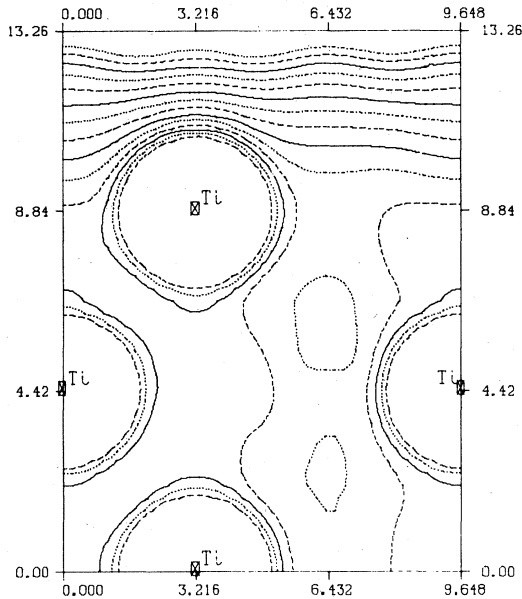


FIG. 2. Contour plot of the charge density of a five-layer Ti(0001) film in a plane normal to the surface and passing through both of what would be the two Ti atoms in the bulk Ti unit cell. The distances are given in a.u. The outermost contour corresponds to a charge density of 2.0×10^{-3} electrons/a.u.³, and adjacent contours differ in charge density by a factor of 1.3. The outermost contours show moderate Gibbs (unphysical, basis-set dependent) oscillations.

the linear combination of localized orbitals form

$$\Psi_{k_{\parallel}}(\vec{r}) = \sum_{\vec{R}_{\parallel}, l, m} c_{\vec{R}_{\parallel}, l, m}^{n, l, m}(\vec{R}) \Phi_{n, l, m}(\vec{r} - \vec{R}) , \quad (1)$$

$$\Phi_{n, l, m}(\vec{r} - \vec{R}) \equiv \frac{1}{N^{1/2}} \sum_{\vec{R}_{\parallel}} e^{i\vec{k} \cdot \vec{R}_{\parallel}} u_{n, l, m}(\vec{r} - \vec{R} - \vec{R}_{\parallel}) . \quad (2)$$

Here the $\Phi_{l, m}(\vec{r} - \vec{R})$ are two-dimensional Bloch functions based on the localized orbitals $u_{n, l, m}$ which are labeled as atomic wave functions. The sum on \vec{R}_{\parallel} in Eq. (2) runs over the sites in the two-dimensional Bravais lattice while the sum on \vec{R} in Eq. (1) runs over a set of sites within the two-dimensional unit cell. In the Ti calculations reported here, the set of \vec{R} 's includes the locations of all the Ti nuclei in the unit cell (11 of them for an 11-layer film) and in addition two sites on either side of the film, 1.1 a.u. directly above the surface layer atoms. These supplementary sites are included in order to allow the electrons additional freedom to spill out into the vacuum. We associate one s and one p_x , p_y , and p_z Gaussian orbital¹² with the supplementary wave-function sites. With each of the Ti nuclear sites we associate two s -, two p -, and two d -like valence electron radial functions.¹³ The procedure for choosing these functions is as follows: Each radial function $R_n(r)$ is initially written as a linear combination of Gaussians,

$$R_n(r) = \sum_{i=1}^{i_{\max}} c_i^n r^i e^{-\alpha_i r^2} , \quad (3)$$

in which the α_i 's are geometrically distributed between 0.03 and 1.2×10^4 a.u., a range which permits variational freedom from distances well within the Ti $1s$ orbital to those sufficiently large to describe a $4s$ state. The c_i 's are then determined by means of an isolated Ti atom calculation. Radial functions for the Ti core orbitals are also taken to be of the form of Eq. (3). Within this basis of Gaussian wave functions the atom Schrödinger equation is solved self-consistently in the local density approximation.¹⁴ The choice of the α_i 's is judged to be adequate by convergence studies. Atomic transition state calculations show that the various Ti ionization potentials are predicted to within ~ 0.5 eV of experimental values.¹⁵

Rather than using the radial functions that are obtained from the self-consistent atom calculation directly for the Ti film wave-function basis, two modifications are made first. Since in an isolated atom the valence wave functions have long tails, inclusion of the contributions of the longest range α_i 's in the expansion of the $R_n(r)$ is likely to lead to overcompleteness problems rather than to increased accuracy. Thus we re-solve the isolated atom Schrödinger equation non-self-consistently using the self-consistent potential previously obtained, but elim-

inating the terms involving the two smallest α_i 's in the basis for the radial functions. (The smallest α_i retained was thus 0.19 a.u.) The radial functions so obtained are guaranteed to be accurate self-consistent wave functions within each Ti atomic cell, but are limited in radial extent. It was stated above that the valence wave-function basis included two each of s , p , and d radial functions. These are the $4s$, $5s$, $4p$, $5p$, $3d$, and $4d$ wave functions which emerge from the isolated atom problem. The $5s$, $5p$, and $4d$ functions in a Ti^0 calculation are positive-energy wave functions, artificially confined to a region of the size of a Ti atom by the α_i cutoff. They are orthogonal to the $4s$, $4p$, and $4d$ functions and are thus useful to incorporate into the film calculation to provide variational flexibility.

A rigid-core approximation is made, which has been shown to give excellent agreement with the full problem in several tests. The matrix elements of the Hamiltonian and the overlap between Bloch sums (or Bloch layer sums in the case of slabs) are computed for both core and valence functions. The matrix elements of the core-orthogonalized valence functions are then computed in a fully variational fashion. In matrix notation, they can be expressed

$$\begin{aligned} H_{vv}^0 &= H_{vv} - S_{vc}H_{cv} - H_{vc}S_{cv} + S_{vc}H_{cc}S_{cv}, \\ S_{vv}^0 &= S_{vv} - 2S_{vc}S_{cv} + S_{vc}S_{cc}S_{cv}, \end{aligned} \quad (4)$$

where the subscripts v and c denote valence and core blocks of the partitioned matrix. Explicit use of the assumption that the atomic core functions are eigenfunctions of the crystal or slab Hamiltonian can algebraically simplify Eqs. (4), but leads to somewhat less accurate results. The density matrix for the orthogonalized Bloch valence functions is re-expanded into unorthogonalized valence and core form in the process of fitting the charge.

We turn now to the question of the charge-potential basis for Ti. The choice of such a basis is already made at the level of the isolated Ti atom calculation. Since the charge varies as the wave function square it seems clear that a reasonable basis would be a set of Gaussians whose α_i 's were double the α_i 's in the wave-function basis. However it is important to make allowance for the singular nature of the screened nuclear potential at $r \rightarrow 0$. Accordingly in the potential basis we include not only a set of Gaussians, $\{e^{-\alpha_i r^2}\}$, but also one additional term of the form $e^{-\alpha_0 r^2}/r$, where α_0 is given a value of $\sim 10^2$ a.u. to simplify multicenter integral summations in the bulk or film. The inclusion of the Gaussian screened Coulomb term in the potential basis does increase the expense of the calculation of the Hamiltonian matrix, but less than would the attempt to fit the r^{-1} potential by having only Gaussians but more of them. In the Ti atom calculation 20 α_i 's are used

geometrically distributed between 0.04 and 2.4×10^4 a.u. Of this set, the value $\alpha = 88.6$ is assigned to the Gaussian screened Coulomb term.

It is important to calculate the electronic structure of bulk hcp Ti as a preliminary step before proceeding to the film calculation. This not only allows us to test both sets of basis functions, but provides a completely parallel self-consistent band structure to aid in interpreting the surface results. For bulk Ti we defined a charge-potential basis as follows: Consider three lines parallel to the c axis. Two of the lines pass through the two Ti atoms in the hcp unit cell, while the third passes through the octahedral interstitial sites.¹⁶ Along each of these lines we center Gaussians every $\frac{1}{4}c$, starting in a plane containing a Ti nucleus. To sites that coincide with a Ti nucleus we assign the same set of Gaussians as we used successfully in the atomic Ti calculation, except that the two longest-ranged Gaussians are omitted because they would lead to overcompleteness in the solid. With all the other sites we associate three Gaussians with α 's equal to 0.327, 0.658, and 1.32 a.u. These relatively long-ranged Gaussians are included to permit charge to flow into the bonding regions of the Ti solid. With this basis, we find that an unconstrained fit to the self-consistent exact Ti charge density gives overall charge neutrality to $\sim 0.01\%$, and a bulk Ti band structure (see Fig. 3) that is quite similar to that of Jepsen,¹⁷ which agrees with Fermi-surface data. (Our band structure differs from that of Jepsen in some details; but differences are to be expected since Jepsen's calculation is non-self-consistent while ours is self-consistent.)

In order to select an adequate basis for the charge and potential just outside a Ti film, we proceeded from the bulk Ti calculation to that of a three-layer (0001) film. In such a film there are only three Ti atoms per unit cell, and consequently numerical experimentation is still relatively inexpensive. The charge-potential basis that was finally adopted for the three-layer film involved the use of the same fitting sites and Gaussians for the interior of the film as were used in the bulk Ti calculation. Outside the film we added additional sites along the three lines parallel to the c axis defined above, at distances of $\frac{1}{16}(3nc)$ above the surface atomic layer, with $n = 0, 1, 2, 3, 4$, and 5. Two Gaussians were associated with each of these sites with α 's of 0.162 and 0.327 a.u. The α 's of 0.658 and 1.32 that were included at the non-nuclear sites in the Ti bulk were dropped in the surface sites because no large variation on this short a scale is expected outside the surface. Although (cf. Fig. 2) the charge fit obtained using this basis could certainly be improved upon, i.e., the unphysical "Gibbs oscillations"¹⁸ in the valence charge density appear already when it has only dropped to $\frac{1}{20}$ its bulk average value, the fact

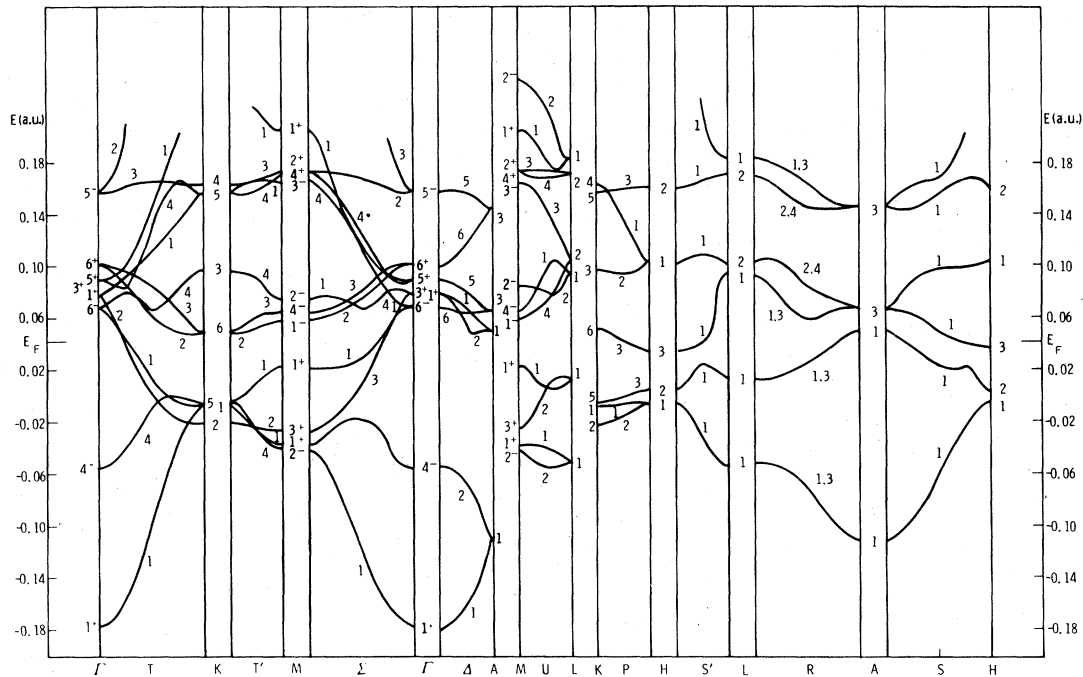


FIG. 3. Self-consistent nonrelativistic bulk band structure of hcp Ti.

that the work function obtained using this charge density differs from experiment⁷ by only 0.2 eV suggests that the basis is adequate. We assumed an unreconstructed, unrelaxed geometry for the Ti film, in accordance with low-energy electron diffraction (LEED) data and calculations.¹⁹

Having found a reasonably good basis to describe a three-layer film the modifications necessary to expand to a thicker film are obvious; one uses the same basis outside and on the surface, and the bulk basis in the interior.

The last technical matter that must be discussed is how we solve the Schrödinger equation for a film as thick as 11 layers. It is important to carry out calculations for such a thick film if one wishes to obtain a description of surface states in which interference between the surface states corresponding to the opposite sides of the film does not occur and split them in energy. In addition for thinner films it is often not easy to determine which states actually are the surface states, because there is not enough bulk region for their wave functions to decay to zero.

Since an 11-layer Ti(0001) film has 11 Ti atoms per unit cell, and thus our wave-function basis involves the solution of a 206×206 generalized eigenvalue problem,²⁰ it is clear that a self-consistent calculation of such a film would be extremely time consuming. However to obtain an approximately self-consistent description of the 11-layer film is quite

straightforward. The idea is to take advantage of the rapid "healing" of the potential as a function of depth below the outer atomic layer. In order to make this idea quantitative we compare the intracenter layer Hamiltonian matrix elements, as well as those between the 2nd and 3rd, and 2nd and 4th layers of a self-consistent five-layer film, with the corresponding matrix elements for what we will call a "bulk Ti film." Clearly it is not trivial to compare the Hamiltonian matrix for a five-layer Ti film numerically with that for bulk Ti, because k_z is a good quantum number for the latter geometry but not for the former. Thus we imagine the case of a Ti film in which the potential energy is fixed to equal that of self-consistent bulk Ti shifted by a constant,²¹ i.e., the charge is not allowed to relax to its self-consistent form for the film. The Hamiltonian matrix for this potential must represent the properties of bulk Ti. But since it has been evaluated as though a film calculation were being performed, only k_x and k_y are treated as good quantum numbers. Thus the "bulk film" Hamiltonian matrix is easy to compare with that of an actual film. The comparison of the five-layer film's interior layer matrix elements with the corresponding elements of a five- or seven-layer "bulk film" reveals agreement to within $\sim 1\%$. This continues to hold true after core orthogonalization. Thus we "stretch" the Hamiltonian matrix of a self-consistent 5-layer film to that of an 11-layer film which is self-consistent to an excel-

lent approximation by filling in the blocks of the matrix corresponding to interior layers with appropriate blocks of the "bulk film" Hamiltonian.

This completes our description of the novel technical features of the Ti film calculation. We turn now to a discussion of the results.

III. CALCULATED STATES OF AN ELEVEN-LAYER Ti(0001) FILM

As noted in the Introduction, the most striking result for the Ti film is the prediction of a band of surface states and resonances coincident with the Fermi level, which lies at -0.139 a.u. relative to the vacuum. In this section we describe the angular-momentum character of these surface states and discuss their dispersion. We also take up the question of the possible observation of the Ti surface band via angle-resolved ultraviolet photoemission spectroscopy (ARUPS).

The surface Brillouin zone (SBZ) and the labeling of its symmetry points and lines are shown in Fig. 4. Energies of the states of the 11-layer slab along these lines are plotted in Figs. 5(a) and (b) for even and odd symmetry with respect to the center plane of the slab.

Examination of the wave functions reveals that states which are peaked at the surface exist throughout much of the SBZ. These are indicated by heavy lines in Fig. 5. There is a pair of reasonably strongly surface-peaked states at Γ at -0.14099 a.u. and -0.14074 a.u., but at \bar{k}_{\parallel} values near Γ these surface states are mixed with the bulk Ti bands and thus are only weak surface resonances. To make such statements more quantitative, we compare the orbital

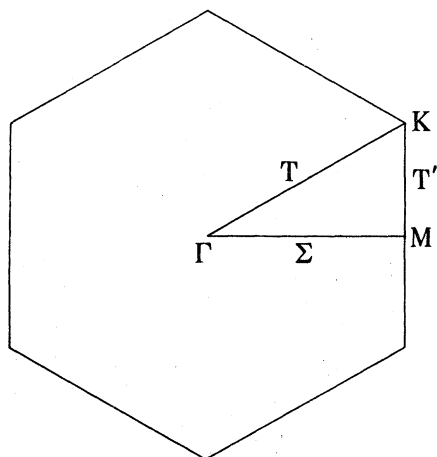


FIG. 4. Two-dimensional Brillouin zone (2-D BZ) for the hcp (0001) surface.

populations²² in the surface layer and averaged over the three central layers of the film,²³ for the wave functions of the surface resonance states. For the surface states at Γ , the surface to bulk population ratios are 30 and 90 for the states at -0.14099 and -0.14074 a.u., respectively; however for the states near the Fermi level and for k_{\parallel} one-sixth of the way from Γ to M the most surfacelike state shows a surface-bulk ratio of ~ 6 , and for k_{\parallel} one-eighth of the way from Δ to K the maximum surface-bulk ratio is 7. Thus the Γ surface state retains its identity over too small a portion of the SBZ to be of physical significance.

On the other hand, a band of well defined surface states splits off the top of the second band continuum approximately half way out along the Γ - Σ - M and Γ - T - K lines, and exists over most of the outer portion of the SBZ. In the vicinity of K , this band of states merges into the third band continuum to become a surface resonance. Approaching the K point itself, however, this resonance sharpens and becomes a true surface state again at K , lying at -0.1386 a.u. This is possible because of the additional symmetry of the K point. The surface state has the symmetry of bulk P_1 and P_2 states,²⁴ while the continuum in which it is embedded is composed of P_3 symmetry states (cf. Fig. 3). Thus the continuum cannot mix with and broaden the surface state. This state is near the middle of a gap between P_1 and P_2 continua, approximately 1.5 eV from the nearest such band edge. As a result, the evanescent tail of the surface state wave function is very rapidly decaying, making it more localized at K than anywhere else in the SBZ. The surface-bulk population ratio is 3.3×10^4 . This band of surface states and resonances is quite flat and straddles the Fermi energy. It contributes the peak in the surface LDOS shown in Fig. 1. The band should be empty around its maximum at M , and occupied elsewhere with one possible exception. At K , the surface state connected with this band lies just at the Fermi energy, and it is not possible to say with certainty whether it is occupied or not within the accuracy of the calculation.

There is another surface state at K of P_3 symmetry, lying in the ~ 1 eV gap between the lowest P_3 bulk bands, at -0.1666 a.u. This state exists over only a small portion of the SBZ and, like the previously discussed state at Γ , will contribute little to physically interesting surface properties.

It should be pointed out that there exist higher surface bands in addition to those near the Fermi energy. But in view of the local orbital nature of our calculation, we do not consider states within an eV or so of the vacuum level to be accurately described, and so do not discuss them further.

The angular-momentum character of the Ti surface band is illustrated in Figs. 6–9. Note that the peak at E_F is absent in the $3z^2 - r^2$ partial LDOS, while it is

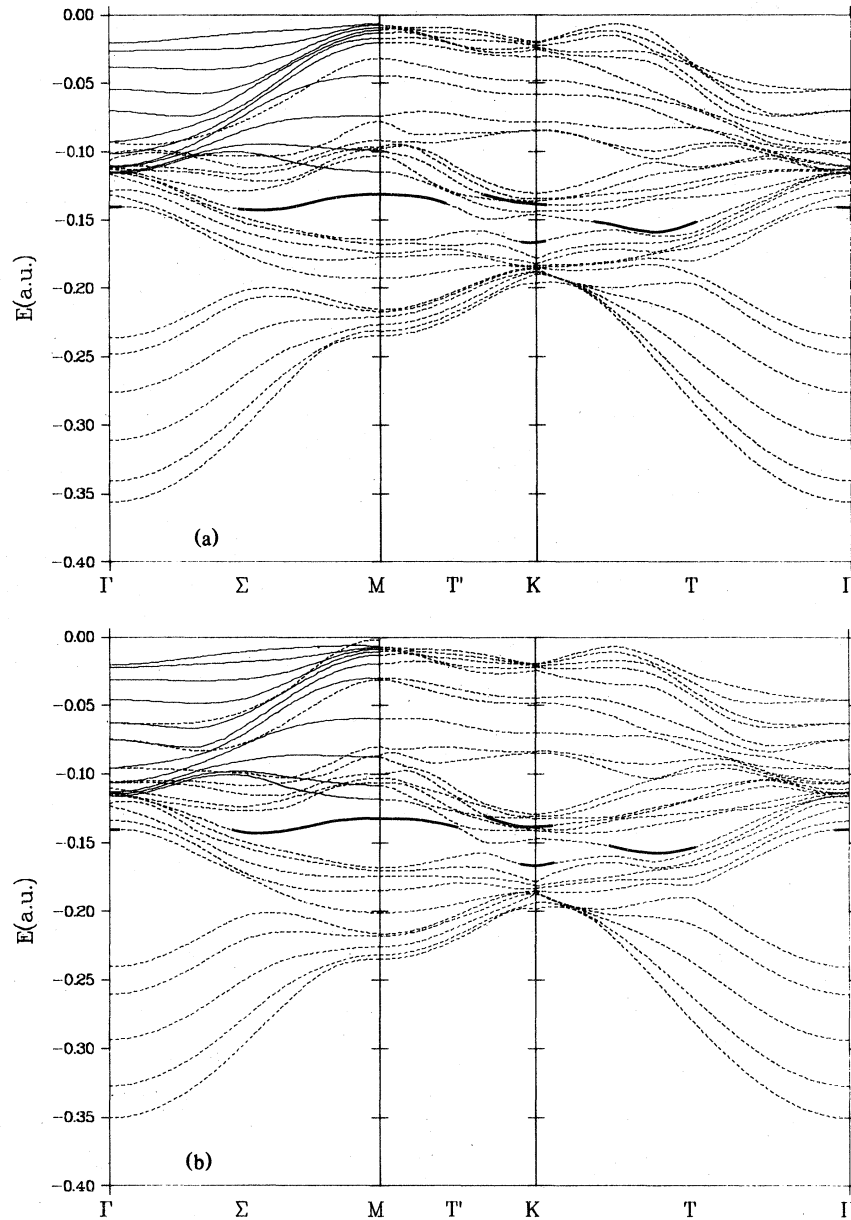


FIG. 5. Two-dimensional band structure for the 11-layer Ti film. Panels (a) and (b) correspond, respectively, to states which are even and odd under reflection in the central plane. The line Γ - Σ - M is a symmetry line. The dashed and solid dispersion relations for this line accordingly represent states which are even and odd under reflection in a plane normal to the surface and passing through the Γ - M line. States near the Fermi level (which is at -0.139 a.u.) that are strongly surface-peaked are indicated by heavy dispersion curves.

strong in the (xz, yz) and $(xy, x^2 - y^2)$ partial LDOS's.²² Near the M - T' - K line the surface states are predominantly of this character. The large surface peak in the s - p partial LDOS, in Fig. 9, does not give a fair indication of the relative s - p character of the surface band. Most of this peak is from wave functions centered on the supplementary fitting sites

outside the outer Ti atomic layer (cf. Sec. II). While these are s - p in symmetry relative to their center, it is difficult to know how to decompose this partial LDOS in an angular-momentum breakdown about the surface atom. It presumably has significant d character.

We turn finally to the question of the possible ob-

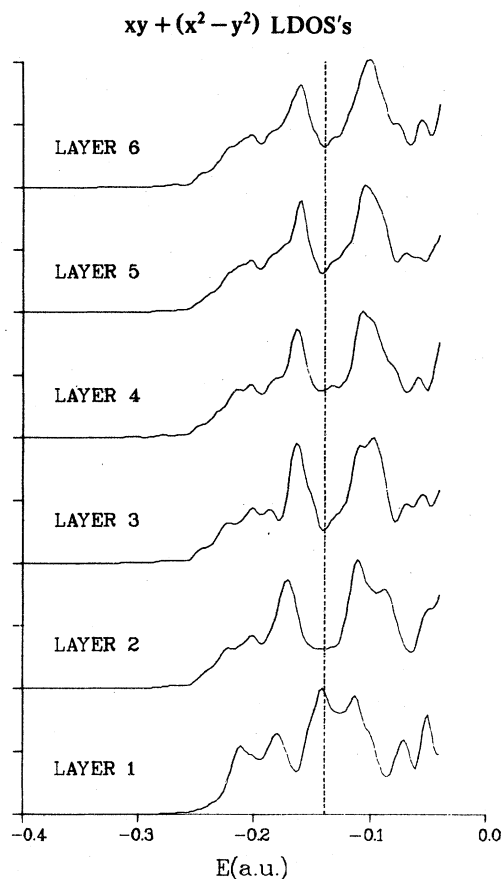


FIG. 6. Local $(xy, x^2 - y^2)$ density of states vs layer. Note the strong surface resonance which coincides with the Fermi level (dashed line) at -0.139 a.u.

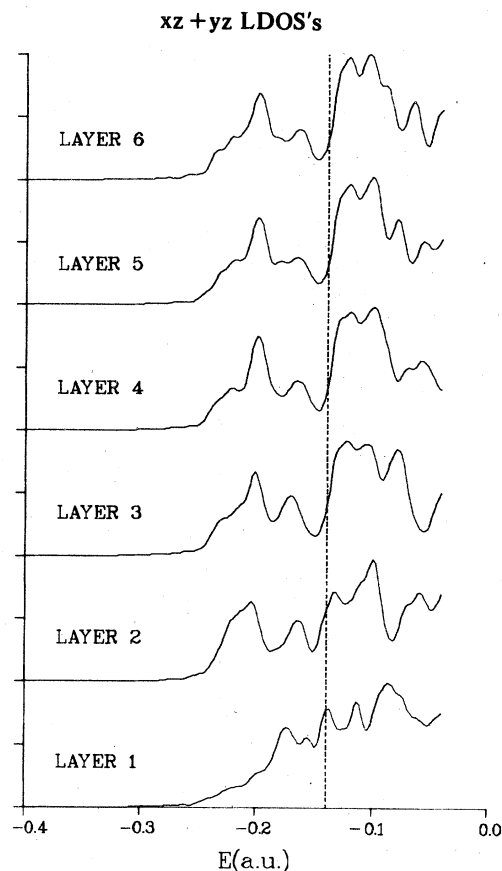


FIG. 7. Local (xz, yz) density of states vs layer. Again the surface resonance at the Fermi level (dashed line) appears strongly in the surface layer. The scale on the ordinate is identical to that in Figs. 6, 8, and 9.

servation of the Ti surface band. Early UPS data of Eastman²⁵ does not show a peak at the Ti Fermi energy. However in this experiment there was rather severe contamination of the Ti sample by H , as evidenced by a large peak ~ 5 eV below the Fermi energy, which increased with the addition of H_2 . Moreover the Ti in the experiment was polycrystalline, and we can make no statement regarding Ti surface states on other than the (0001) face.

Recent unpublished results of Rabalais and Ignatiev²⁶ for apparently clean Ti(0001) show what may be a surface state²⁷ about 1 eV below the Fermi level. This peak, however, mysteriously disappears above 160°C , which is not understood.

Unfortunately the selection rules for angle-resolved photoemission²⁸ do not distinguish surface from bulk states for the Ti(0001) surface. These selection rules apply only when the parallel component of the photoelectron wave vector is zero or lies along a mirror plane, i.e., for an hcp (0001) surface, only along the

line Γ - Σ - M in the SBZ.

At Γ , i.e., for electrons exiting along the surface normal, a glance at the bulk band structure (Fig. 3) shows that all the occupied states are of the same symmetry Δ_1 and Δ_2 , and thus are invariant to rotations of $\pm 120^\circ$ about the c axis.²³ Thus at Γ no states should be seen at normal incidence, and all the states should increase in intensity (depending on their photoemission matrix elements) for p -polarized light as the angle of incidence increases off-normal.

At M , as along the line Γ - Σ - M , the only symmetry operation for the Ti film is reflection across the Γ - M axis, and all the occupied states are even under this reflection [cf. Figs. 5(a) and (b)]. Thus for light whose \vec{E} vector is in the plane of the surface perpendicular to the Γ - M direction no photoemission should be seen for any \vec{k}_\parallel along Γ - M . On the other hand as \vec{E} is rotated into the Γ - M direction or is rotated out of the surface plane, photoemission should be seen.

It is at the K point in the SBZ that surface and

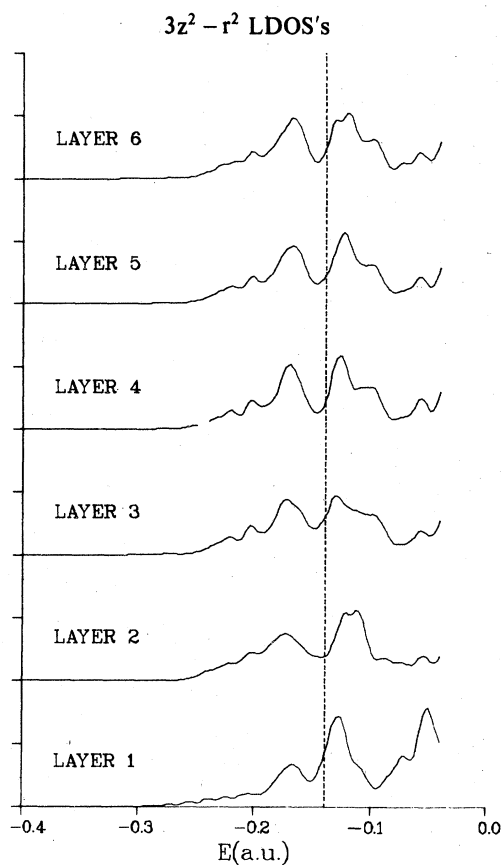


FIG. 8. Local $3z^2 - r^2$ density of states vs layer. Here the surface resonance near the Fermi level is so weak that it cannot be resolved. The scale on the ordinate is the same as in Figs. 6, 7, and 9.

bulk states of different symmetries lie in the same energy range. However recalling that the final electron wave function in a photoemission matrix element contains a single outgoing plane wave in the direction of the detector and otherwise only ingoing plane waves, it is obvious that at K the final electron wave function does not have any special symmetry quantum number. Consequently orientation of the photon polarization vector will not permit one selectively to enhance the bulk or surface states at K .

IV. DISCUSSION

The surface density of states for Ti(0001) is strongly modified in the lower portion of the d band. In the bulk, the Fermi level lies at a minimum between two peaks in the DOS, while at the surface these peaks appear to merge and sharpen, with the new maximum falling just at E_F , as shown in Fig. 1. The fact that the surface LDOS peak falls at the bulk minimum is closely related to the fact that the peak is composed primarily of surface state contributions.

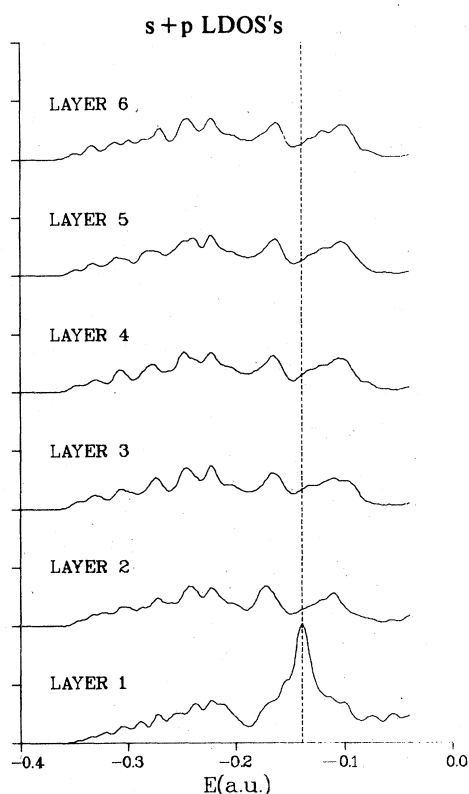


FIG. 9. Local $s-p$ density of states vs layer. The scale on the ordinate is the same as in Figs. 6, 7, and 8. The surface resonance at the Fermi level (dashed line) is very strong. However, most of this peak comes from the supplementary wave-function fitting site we have placed outside the outer Ti atomic layer. Consequently it would be incorrect to deduce from this figure that the surface band is heavily $s-p$ -like.

The bulk DOS minimum reflects a low concentration of bands in this energy range, which results in a large gap region in the projected bulk band structure.

Narrowing of the surface density of states is commonly anticipated from a simple argument based on a one-state nearest-neighbor tight-binding model: The mean-square bandwidth (second moment) is proportional to the number of neighbors, so reduced coordination at the surface implied reduced bandwidth. Calculations for the (111) surfaces of fcc Cu and Pd, which have local geometry similar to (0001) hcp Ti, do show such narrowing.^{5,6} In these cases, the d -band DOS falls well below the vacuum level, and can be isolated to permit a second-moment calculation. The second-moment decrease found in Cu and Pd is somewhat smaller than that predicted from neighbor counting.

For Ti(0001) the narrowing and peaking of the surface DOS near E_F involves only the lower d bands, and is qualitatively different from the narrowing discussed above for Cu and Pd. The top of the Ti d

band falls slightly above the vacuum level, so the present calculations cannot give dependable results for the upper portions of these bands. It is the second moment of the complete set of bands which is supposed to narrow by the neighbor effect, and this is determined primarily by the band extremes. The rearrangement of weight near E_F , while dramatic compared to the Cu and Pd results, may have little effect on the second moment. If it had been possible to examine the d -band second moment we expect that a degree of narrowing comparable to that found for Cu and Pd (111) would have been found.

The other two metals from the left side of the transition series for which self-consistent surface calculations have been carried out are Nb (Ref. 3) and Mo (Ref. 4). Both calculations were for the (100) face of these bcc materials, so the analogy with the present case is not strong. However, for Nb the surface DOS is maximum in the first major minimum of the bulk DOS, with a number of surface states and resonances contributing. The Fermi level lies just below the bulk DOS minimum; so while there is some surface enhancement of the Fermi level DOS at the surface, most of these surface state bands are empty. In Mo, there is also surface enhancement of the DOS in the corresponding bulk minimum. In this case, E_F lies within the minimum, and several bands of surface states and resonances occur at E_F .

A major question raised in the current results is the interplay between self-consistency and the surface spectrum. The partially occupied surface state band of Ti(0001) seems to play a significant role in determining the surface dipole. It is not clear whether this should be expected to hold for other hcp (0001) metal surfaces. For Sc, with one less electron than Ti, a rigid-band picture would suggest that the corresponding surface states should be predominantly unoccupied. Whether this is true, or whether the spectrum changes significantly and the rigid-band picture breaks down, remains to be seen. In the former case, we would expect a substantial decrease in the surface dipole. The Nb,³ and Mo,⁴ results suggest rigid-band behavior with respect to the analogous surface DOS features, but work functions and dipoles have not been calculated. Furthermore, the geometric differences may be too great to draw any inferences about the present case.

Core-level shifts at surfaces are another interesting consequence of the self-consistent surface potential. In a similar previous calculation for Cu(111), the surface core levels were found to be shifted upward relative to the bulk (in the direction of lesser absolute binding energy) by ~ 0.5 eV. An upward surface core shift of 0.4 eV has recently been found experimentally for Au polycrystalline films.²⁹ In the present work, we find a *downward* shift (direction of greater absolute binding energy) of 0.25 eV at the Ti(0001) surface.

This retrograde core shift is, in fact, consistent with a simple physical picture of surface self-consistency for transition metals. Let us neglect the s - p electrons, and imagine that the d -band surface LDOS is simply a narrowed version of the bulk DOS. Since the Fermi level is pinned by the bulk, the center of gravity of the surface LDOS will also have to change to preserve charge neutrality at the surface. For a more than half-filled d band, the center of gravity must shift upward at the surface, while for a less than half filled band it should shift downward. The shift is accomplished by an electrostatic screening potential, which is felt equally by the core levels.

The assumptions of the above arguments are sufficiently naive that it is somewhat surprising to see even the predicted trend borne out in the few calculations that have examined this effect. Strict application of the argument to Cu and Au would suggest no effect, since the d band is filled. However, s - d hybridization should break down this strict exclusion.²⁹ For both the Cu calculation and the Au experiment, the surface d -band centers of gravity were computed, and found to shift essentially the same amount as the core levels. This gives further support to the screening potential mechanism for the core shifts.

Another plausible model predicting the direction of the surface core shift can be given. In this model, we simply compare the bulk and atomic core levels (relative to the vacuum), and argue that a surface atom should be somewhat more like a free atom. For Ti, the atom core levels are 2.3 eV lower than the bulk levels, and the surface core levels are 0.25 eV lower. For Cu(111) on the other hand, the atom and surface levels are 2.6 and 0.5 eV higher, respectively. We must be careful to note that these differences refer to the core eigenvalues calculated within the local exchange-correlation potential approximation for the free atom, surface atom, and solid. Measured core energies are shifted by relaxation effects, and while intra-atomic relaxation should be the same in all cases, the inter-atomic relaxation present (and presumably equal) for the bulk and surface atoms is absent for the free atom.³⁰ Thus experimentally measured core levels should not in general follow the bulk-surface free-atom trend unless the inter-atomic relaxation can be accurately estimated and subtracted.

ACKNOWLEDGMENTS

We wish to thank P. H. Citrin for useful conversations concerning surface core-level shifts. The portion of this work performed at Sandia Laboratories was supported by the U.S. DOE under Contract No. AT(29-1)-789.

*A. U. S. Department of Energy facility.

¹J. G. Gay, J. R. Smith, and F. J. Arlinghaus, *Phys. Rev. Lett.* **38**, 561 (1977); J. A. Appelbaum and D. R. Hamann, *Solid State Commun.* **27**, 881 (1978).

²J. A. Appelbaum and D. R. Hamann (unpublished); O. Jepsen (unpublished).

³S. G. Louie, K. M. Ho, J. R. Chelikowsky, and M. L. Cohen, *Phys. Rev. Lett.* **37**, 1289 (1976); *Phys. Rev. B* **15**, 5627 (1977).

⁴G. P. Kerker, K. M. Ho, and M. L. Cohen, *Phys. Rev. Lett.* **40**, 1593 (1978).

⁵S. G. Louie, *Phys. Rev. Lett.* **40**, 1525 (1978).

⁶J. A. Appelbaum and D. R. Hamann, *Solid State Commun.* **27**, 881 (1978).

⁷J. R. Anderson and N. Thompson, *Surf. Sci.* **26**, 397 (1971), obtained 3.95 eV. Similar values have been obtained by many others, as reviewed by R. J. D'Arcy and N. A. Surplice, *Surf. Sci.* **36**, 783 (1973). However these latter authors believe that a higher value, ~4.2–5.6 eV, is more characteristic of clean Ti.

⁸See also J. A. Appelbaum and D. R. Hamann, Ref. 1.

⁹I.e., sums of Gaussians.

¹⁰H. Sambe and R. H. Felton, *J. Chem. Phys.* **62**, 1122 (1975). See also, K. Mednick and C. C. Lin, *Phys. Rev. B* **17**, 4807 (1978).

¹¹These are essentially the Gibbs oscillations, which arise from trying to fit a charge distribution with a basis that contains only a finite set of "Fourier components," or in the Gaussian case, attenuation constants.

¹²These orbitals are of the form $\exp(-1.5 \text{ a.u.} \times r^2)$ times 1 for the *s* orbital and times *x*, *y*, and *z* for the respective *p* orbitals.

¹³Thus for an 11-layer Ti film the Hamiltonian matrix is 206×206 . The number 206 is 2×4 for the supplementary sites plus 11×18 for the Ti nuclear sites.

¹⁴The local exchange-correlation potential is taken to be that of the Wigner interpolation formula. See D. Pines, *Elementary Excitations in Solids* (Benjamin, New York, 1963), Eq. (3.58).

¹⁵C. E. Moore, *Atomic Energy Levels*, N.B.S. Circular No. 467 (U. S. GPO, Washington, D.C., 1949). Since spin is not included in our calculations we compare to experimental ionization potentials which are spin averaged.

¹⁶Choosing to place a Ti atom at (0,0,0) and defining the lattice vectors to be $\frac{1}{2}a(1, \pm 3^{1/2})$ and (0,0,*c*), the octahedral sites in the unit cell lie at $(\frac{1}{2}a, a/2(3)^{1/2}, \frac{1}{4}c)$ and $(\frac{1}{2}a, a/2(3)^{1/2}, \frac{3}{4}c)$. The second Ti atom in the cell is at $(\frac{1}{2}a, -a/2(3)^{1/2}, \frac{1}{2}c)$. In all our calculations we used $a = 5.57 \text{ a.u.}$, $c = 8.84 \text{ a.u.}$

¹⁷O. Jepsen, *Phys. Rev. B* **12**, 2988 (1975).

¹⁸Cf., Ref. 11.

¹⁹According to low-energy electron diffraction results, the Ti(0001) surface is 1×1 and the outer layer is relaxed inward by ~2%; see H. D. Shih, F. Jona, D. W. Jepsen, and P. M. Marcus, *J. Phys. C* **2**, 1405 (1976).

²⁰The problem is a "generalized" eigenvalue problem because our basis of valence wave functions is not orthogonalized. The calculation of the number 206 is explained in Ref. 13.

²¹That is, we define a set of potential fitting sites for the bulk film which consists of the sites used in the bulk Ti calculation, extended out several layers on either side of the film, and assign to each Gaussian the coefficient of the corresponding Gaussian obtained in the self-consistent bulk results.

²²We calculate populations and local densities of states by a method akin to the Mulliken population analysis, proposed by D. G. Dempsey and L. Kleinman, *Phys. Rev. B* **16**, 5356 (1977). If the Schrödinger equation is written in the form

$$\sum_{n',l'} [H_{l,n;n'l'}(\vec{k}_{\parallel}) - E_b(\vec{k}_{\parallel})S_{n,l;n'l'}(\vec{k}_{\parallel})]c_{n',l'}^b(\vec{k}_{\parallel}) = 0,$$

where *b*, *l*, and *n* are, respectively, band, layer, and orbital indices, and where $S_{n,l;n'l'}$ is the overlap matrix, which is not $\delta_{nn'}\delta_{ll'}$ because of the use of nonorthogonal basis functions, then the local density of states in the *l*th layer is defined to be

$$\rho_l(E) = \sum_b \sum_{\vec{k}_{\parallel}} \sum_{n,n'} \sum_{l'} \delta(E - E_b(\vec{k}_{\parallel})) \times \text{Re}[c_{n,l}^b(\vec{k}_{\parallel})^* S_{nl,n'l'} c_{n',l'}^b(\vec{k}_{\parallel})]$$

This definition shares the "bonding" (i.e., interlayer) charge between the atoms at the ends of a bond, and is guaranteed to add to the total density of states when summed on *l*. The partial LDOS's are defined similarly, by restricting the *n* (but *not* the *n'*) sum to the orbitals of interest.

²³Since the film is symmetric under reflection in its central layer, the LDOS in the central layer alone does not give an accurate portrayal of the amplitude of a state in the bulk.

²⁴The symmetry properties of the hcp (0001) surface are easy to derive from Slater's tabulation for a bulk hcp crystal. See J. C. Slater, *Quantum Theory of Molecules and Solids* (McGraw-Hill, New York, 1965), Vol. 2. Note that for the film the P_1 and P_2 representations are indistinguishable.

²⁵D. E. Eastman, *Solid State Commun.* **10**, 933 (1972).

²⁶W. N. Rabalais and A. Ignatiev (private communication).

²⁷According to the test of sensitivity to adsorption.

²⁸J. Hermanson, *Solid State Commun.* **22**, 9 (1977).

²⁹P. H. Citrin, G. K. Wertheim, and Y. Baer, *Phys. Rev. Lett.* **41**, 1425 (1978).

³⁰L. Ley, S. P. Kowalczyk, F. R. McFeely, R. A. Pollak, and D. A. Shirley, *Phys. Rev. B* **8**, 2392 (1973); P. Citrin and D. R. Hamann, *Chem. Phys. Lett.* **22**, 301 (1973), and *Phys. Rev. B* **10**, 4948 (1974); R. E. Watson, M. L. Perlman, and J. F. Herbst, *Phys. Rev. B* **13**, 2358 (1976); A. R. Williams and N. D. Lang, *Phys. Rev. Lett.* **40**, 954 (1978).